High entropy leads to symmetry equivariant policies in Dec-POMDPs

Johannes Forkel [1] **Constantin Ruhdorfer** [2] **Andreas Bulling** [2] **Jakob Foerster** [1]

Abstract

We prove that in any Dec-POMDP, sufficiently high entropy regularization ensures that policy gradient ascent with tabular softmax parametrization always converges, for any initialization, to the same joint policy, and that this joint policy is equivariant w.r.t. all symmetries of the Dec-POMDP. In particular, policies coming from different random seeds will be fully compatible, in that their cross-play returns are equal to their self-play returns. Through extensive empirical evaluation of independent PPO in the Hanabi, Overcooked, and Yokai environments, we find that the entropy coefficient has a massive influence on the cross-play returns between independently trained policies, and that the drop in self-play returns coming from increased entropy regularization can often be counteracted by greedifying the learned policies after training. In Hanabi we achieve a new SOTA in inter-seed cross-play this way. Despite clear limitations of this recipe, which we point out, both our theoretical and empirical results indicate that during hyperparameter sweeps in Dec-POMDPs, one should consider far higher entropy coefficients than is typically done.

1. Introduction

Training agents that can coordinate well with novel partners is a central problem in multi-agent reinforcement learning (MARL). When using *self-play* (SP) to train a joint policy in a decentralized partially observable Markov decision process (Dec-POMDP), this typically results in the joint policy adopting a coordination convention which breaks symmetries of the Dec-POMDP. When agents from such a joint policy are then paired in *cross-play* (XP) with agents from another joint policy which wasn't seen during training, e.g. with a joint policy trained with the same algorithm but a different random seed, a wholly different algorithm, or with humans, this can result in coordination failures, since the coordination conventions of the different joint policies are incompatible with each other. For a simple example of such incompatible symmetry breaking, consider the one-round simultaneous action game with the common pay-off matrix

$$\begin{bmatrix} 2 & -2 & 1 \\ -2 & 2 & 1 \\ 1 & 1 & 1 \end{bmatrix}. \tag{1}$$

In this Dec-POMDP both joint policies which are optimal in SP break the symmetry in opposing ways: either both local policies always choose the first action, or both always choose the second action, for a SP return of 2. Those two joint policies are incompatible though, in that their XP return is -2: when a local policy from one of those joint policies is paired with a local policy of the other joint policy, then this gives a return of -2. Given that one cannot deduce a preference for either one of those joint policies from the Dec-POMDP, the average XP return in a large population of SP optimal policies will be 0. This is lower than 1, which is the average XP return between any number of optimal symmetry equivariant joint policies, under which both local policies always choose the third action.

In large and complex Dec-POMDPs like Hanabi (Bard et al., 2020) and Overcooked (Carroll et al., 2019), standard MARL algorithms like independent PPO (IPPO) or independent DQN, have been reported to produce joint policies which, while achieving high returns in SP, do very poorly when paired in XP between independent seeds of the same algorithm (Hu et al., 2020; Bard et al., 2020; Gessler et al., 2025), and in XP with human proxy bots (Dizdarević et al., 2025). This is because those algorithms are unconstrained in which of the many different conventions they can converge to, and thus mostly converge to conventions which break symmetries of the Dec-POMDP.

We prove that, even without any prior knowledge of the symmetries of the Dec-POMDP, tabular softmax policy gradient ascent with sufficiently high entropy regularization will always converge, for any initialization, to a unique joint policy which is equivariant w.r.t. all symmetries of the Dec-POMDP. This is true both when using exact gradient or unbiased estimates thereof. Thus, for sufficiently high entropy regularization, policies from different random seeds

[1]FLAIR, Department of Engineering Science, University of Oxford, United Kingdom [2]Collaborative Artificial Intelligence, University of Stuttgart, Germany. Correspondence to: Johannes Forkel <johannes.forkel@eng.ox.ac.uk>.

Preprint. February 19, 2026.

will be fully compatible with each other, in that their SP returns are equal to their XP returns.

We find that this theoretical insight carries over into practice, where the drop in SP returns coming from high entropy regularization can often be counteracted by greedifying the policies after training. Using standard IPPO implementations in Hanabi and Overcooked, we achieve high inter-seed XP as we increase the entropy regularization, with SP and XP being equal. In Hanabi in particular, IPPO with an entropy coefficient of 0.05 achieves a new SOTA in inter-seed XP, surpassing all previous highly specialized algorithms (Hu et al., 2020; Cui et al., 2021; Hu et al., 2021; Cui et al., 2022; Lupu et al., 2021; Muglich et al., 2022; 2025) by a significant margin. All other PPO hyperparameters we use are fairly standard, with the main difference being a significantly higher entropy coefficient.

While the recipe of high entropy regularization during training and greedification after training will produce symmetry equivariant policies, the resulting policies might be very poor in SP, even among the symmetry equivariant policies. We show that in two simple toy games, as well as in the recently published Yokai learning environment (Ruhdorfer et al., 2025), that when the entropy regularization is high enough to ensure that all seeds converge to the same policy, that the resulting policy, even when greedified, is extremely poor, and in the case of the two toy environments provably suboptimal among the symmetry equivariant policies.

To summarize, we show both theoretically and through extensive empirical experiments, that through high entropy regularization alone, one can ensure that standard policy gradient methods in Dec-POMDPs will converge to a unique symmetry equivariant policy. We thus argue that when the aim is to learn symmetry equivariant policies, e.g. in order to be able to coordinate with previously unseen other policies, then during hyperparameter sweeps for policy gradient methods one should sweep the entropy coefficient over a far bigger range than is typically done.

2. Background

2.1. Decentralized Partially Observable Markov Decision Processes (Dec-POMDPs)

We formalize the cooperative multi-agent setting as a decentralized partially observable Markov decision process (Dec-POMDP):

Definition 2.1 (Dec-POMDP (Oliehoek et al., 2007))**.** A Dec-POMDP is defined as a 10-tuple $(\mathcal{S}, n, \{\mathcal{A}^i\}_{i=1}^n, \{\mathcal{O}^i\}_{i=1}^n, \mathcal{T}, \mathcal{R}, \{\mathcal{U}^i\}_{i=1}^n, T, \gamma, b_0)$, where:

- $\mathcal{S}$ is the finite state space, b_0 is the initial state distribution, and n is the number of agents.
- $\mathcal{A}^i$ and $\mathcal{O}^i$ are the finite local action and observation spaces for agent i, and $\mathcal{A} = \prod_i^n \mathcal{A}^i$, $\mathcal{O} = \prod_i^n \mathcal{O}^i$ are the joint action and observation spaces.
- $\mathcal{T}(s_{t+1}|s_t, a_t)$ is the probability to transition to state s_{t+1} when taking the joint action $a_t = (a_t^1, ..., a_t^n) \in \mathcal{A}$ in state s_t. $o_t^i := \mathcal{U}^i(s_t) \in \mathcal{O}^i$ is the local observation agent i receives in of state s_t, and we set $\mathcal{U}(s_t) := (o_t^1, ..., o_t^n) \in \mathcal{O}$.
- The rewards are given by $r_{t+1} = \mathcal{R}(s_{t+1}, a_t) \in \mathbb{R}$, the horizon is $T \in \mathbb{N}$, i.e. s_T is always a terminal state, and $\gamma \in [0, 1]$ is the discount factor.

Given $t \in \{0, ..., T\}$, the state-action history (SAH) is given by $\tau_t = (s_0, a_0, ..., s_{t-1}, a_{t-1}, s_t)$. Each agent i selects local actions based on his local action-observation history (AOH) $\tau_t^i = (o_0^i, a_0^i, o_1^i, \dots, a_{t-1}^i, o_t^i)$, following a local policy $a_t^i \sim \pi^i(a_t^i|\tau_t^i)$. Given a SAH τ_t, the local AOHs are deterministic functions of it, and a joint policy $\pi = (\pi^1, \dots, \pi^n)$ chooses a joint action $a_t = (a_t^1, ..., a_t^n) \in \mathcal{A}$, with probability $\pi(a_t|\tau_t) := \prod_{i=1}^n \pi^i(a_t^i|\tau_t^i)$. We denote the set of joint policies by Π, and define the self-play (SP) objective $J_{\text{SP}} : \Pi \to \mathbb{R}$ as the expected return:

$$J_{\text{SP}}(\pi) = \mathbb{E}_{\tau_T \sim \pi}\left[\sum_{t=0}^{T-1} \gamma^t \mathcal{R}(s_{t+1}, a_t)\right]. \tag{2}$$

Furthermore, given π, we define its **greedification** $\hat{\pi}$ by

$$\hat{\pi}(a_t|\tau_t) := \begin{cases} 1/K & \text{if } a_t \in \text{argmax}_{a \in \mathcal{A}} \pi(a|\tau_t), \\ 0 & \text{else,} \end{cases}$$

where here $K := |\text{argmax}_{a \in \mathcal{A}} \pi(a|\tau_t)|$ is the number of joint actions with the highest probability.

2.2. Zero-Shot Coordination (ZSC)

There are typically many joint policies in a Dec-POMDP which maximize the SP return J_{SP}, but those joint policies might be incompatible which each other. The XP return J_{XP}, defined as follows, measures the compatibility between different joint policies in a Dec-POMDP:

Definition 2.2 (Cross-Play (XP))**.** Given a Dec-POMDP with n players, we define the cross-play (XP) return $J_{\text{XP}} : \Pi^n \to \mathbb{R}$, between n joint policies π_1, ..., π_n by

$$J_{\text{XP}}(\pi_1, ..., \pi_n) := \mathbb{E}_{\phi \sim \text{Perm}(n)}\left[J_{\text{SP}}((\pi^1_{\phi(1)}, ..., \pi^n_{\phi(n)}))\right],$$

where $\text{Perm}(n)$ is the set of permutations of $\{1, ..., n\}$.

For example, for $n = 2$, this becomes $J_{\text{XP}}(\pi_1, \pi_2) = \frac{1}{2}[J_{\text{SP}}((\pi_1^1, \pi_2^2)) + J_{\text{SP}}((\pi_2^1, \pi_1^2))]$. Given joint policies $\pi_1, ..., \pi_m$, we refer to the matrix $\left(J_{\text{SP}}((\pi_j^1, \pi_k^2))\right)_{j,k=1}^m$ as the XP matrix of $\pi_1, ..., \pi_m$.

The goal of zero-shot coordination (ZSC), introduced in (Hu et al., 2020), is to find algorithms, which produce compatible joint policies across different implementations, in particular across different random seeds of the same implementation. In Hanabi, ZSC algorithms have led to high XP returns between independently trained joint policies from different random seeds of the same implementation (Hu et al., 2021; Cui et al., 2022), and in XP with human-proxy bots (Dizdarević et al., 2025).

2.3. Symmetries in Dec-POMDPs

Definition 2.3 (Dec-POMDP Symmetries (Hu et al., 2020))**.** Given a Dec-POMDP, a tuple of bijections $\phi := (\phi_{\mathcal{S}}, (\phi_{\mathcal{A}^i})_{i=1}^n, (\phi_{\mathcal{O}^i})_{i=1}^n)$ is a Dec-POMDP symmetry, if

$$\begin{aligned} &\phi_{\mathcal{S}} : \mathcal{S} \to \mathcal{S}, \\ &\phi_{\mathcal{A}^i} : \mathcal{A}^i \to \mathcal{A}^i, \ i = 1, ..., n, \\ &\phi_{\mathcal{O}^i} : \mathcal{O}^i \to \mathcal{O}^i, \ i = 1, ..., n, \end{aligned} \tag{3}$$

are all bijections, and

$$\begin{aligned} \mathcal{T}(s'|s,a) =& \mathcal{T}(\phi_S(s')|\phi_S(s), \phi_A(a)), \ \forall s, s' \in \mathcal{S}, \ a \in \mathcal{A}, \\ \mathcal{U}(s) =& \phi_{\mathcal{O}}^{-1}\left(\mathcal{U}(\phi_S(s))\right), \ \forall s \in \mathcal{S}, \\ \mathcal{R}(s,a) =& \mathcal{R}(\phi_S(s), \phi_A(a)), \ \forall s \in \mathcal{S}, \ a \in \mathcal{A}, \end{aligned} \tag{4}$$

where for joint actions $a = (a^1, ..., a^n) \in \mathcal{A}$, joint observations $o = (o^1, ..., o^n) \in \mathcal{O}$, and SAHs $\tau_t = (s_0, a_0, ..., a_{t-1}, s_t)$, we define $\phi_{\mathcal{A}}(a)$, $\phi_{\mathcal{O}}(o)$, and $\phi(\tau_t)$ by applying $\phi_{\mathcal{S}}$, $\phi_{\mathcal{O}^i}$ and $\phi_{\mathcal{A}^i}$ elementwise. We denote by Φ the set of all Dec-POMDP symmetries of a Dec-POMDP.

Dec-POMDP symmetries act on joint policies in the following way: for $\phi \in \Phi$ and $\pi \in \Pi$, we define the joint policy $\phi(\pi) := (\phi(\pi^1), ..., \phi(\pi^n))$ by the formula

$$\phi(\pi^i)(a^i|\tau^i) := \pi^i(\phi^{-1}(a^i)|\phi^{-1}(\tau^i)). \tag{5}$$

We define a joint policy π to be symmetriy equivariant if $\phi(\pi) = \pi$ for all $\phi \in \Phi$, else we call π symmetry breaking. In order to learn policies which do not break symmetries of the game, Hu et al. (2020) introduced the Other-Play (OP) J_{OP}, defined as follows:

Definition 2.4 (Other-Play (Hu et al., 2020))**.** In a Dec-POMDP the Other-Play (OP) objective J_{OP} is defined as:

$$J_{\text{OP}}(\pi) := \mathbb{E}_{(\phi^1,...,\phi^n)\sim\Phi^n}\left[J_{\text{SP}}((\phi^1(\pi^1), ..., \phi^n(\pi^n)))\right].$$

Maximizing J_{OP} instead of J_{SP} leads to symmetry equivariant policies. For example, in the game with payoff matrix (1), $\Phi = \{\text{Id}, \phi_{1\leftrightarrow 2}\}$ where $\phi_{1\leftrightarrow 2}$ corresponds to permuting the first two actions. Then $\phi_{1\to 2}(\pi_1) = \pi_2$ and $\phi_{1\leftrightarrow 2}(\pi_3) = \pi_3$, where for $j = 1, 2, 3$, π_j denotes the joint policy under which both agents always choose the j-th action. Then $J_{\text{SP}}(\pi_1) = J_{\text{SP}}(\pi_2) = 2 < 0 = J_{\text{OP}}(\pi_1) = J_{\text{OP}}(\pi_2)$, and $J_{\text{SP}}(\pi_3) = J_{\text{OP}}(\pi_3) = 1$. Thus, optimizing for J_{OP} in this game yields the optimal symmetry equivariant policy.

The big drawback of the OP algorithm is that one needs to know the symmetries of the Dec-POMDP a priori. Muglich et al. (2025) provide an algorithm to learn symmetries, which can then be used in the OP objective, but those symmetries are just approximate and the algorithm in Muglich et al. (2025) doesn't guarantee to find all of the Dec-POMDP symmetries. Furthermore, even when knowing all the Dec-POMDP symmetries, there can be multiple incompatible OP optimal policies (Treutlein et al., 2021).

2.4. Entropy Regularized Multi-Agent Policy Gradients

Let $\theta \mapsto \pi_\theta$ be a differentiable parameterization of the joint policy π_θ. For an entropy coefficient $\alpha \geq 0$, we consider the entropy regularized policy gradient

$$\begin{aligned} &\nabla_\theta^\alpha J_{\text{SP}}(\pi_\theta) \\ :=& \nabla_\theta J_{\text{SP}}(\pi_\theta) + \alpha \mathbb{E}_{\tau_T\sim\pi_\theta}\left[\nabla_\theta \sum_{t=0}^{T-1} \gamma^t \text{Ent}(\pi_\theta(\cdot|\tau_t))\right]. \\ =& \mathbb{E}_{\tau_T\sim\pi_\theta}\left[\sum_{t=0}^{T-1}\gamma^t \sum_{i=1}^{n}\left(\nabla_\theta \text{Ent}(\pi_\theta^i(\cdot|\tau_t^i))\right.\right. \\ &\left.\left. + \nabla_\theta \log \pi_\theta^i(a_t^i|\tau_t^i) \sum_{t'=t}^{T-1}\gamma^{t'-t}\mathcal{R}(s_{t'+1}, a_{t'})\right)\right]. \end{aligned} \tag{6}$$

Note that $\nabla_\theta^\alpha J_{\text{SP}}(\pi_\theta)$ is in general **not** the gradient of a function, so in particular not the same as the gradient $\nabla_\theta J_{\text{SP}}^\alpha(\pi_\theta)$ of the maximum entropy reinforcement learning objective

$$J_{\text{SP}}^\alpha(\pi_\theta) := J_{\text{SP}}(\pi_\theta) + \alpha \mathbb{E}_{\tau_T\sim\pi_\theta}\left[\sum_{t=0}^{T-1}\gamma^t \text{Ent}(\pi_\theta(\cdot|\tau_t))\right],$$

because, with $p_{\pi_\theta}(\tau_T) := \prod_{t=0}^{T-1}\pi_\theta(a_t|\tau_t)\mathcal{T}(s_{t+1}|s_t, a_t)$,

$$\begin{aligned} &\nabla_\theta J_{\text{SP}}^\alpha(\pi_\theta) - \nabla_\theta^\alpha J_{\text{SP}}(\pi_\theta) \\ =& \mathbb{E}_{\tau_T\sim\pi_\theta}\left[\sum_{t=0}^{T-1}\nabla_\theta \log \pi_\theta(a_t|\tau_t) \sum_{t'=t+1}^{T-1}\gamma^{t'}\text{Ent}(\pi_\theta(\cdot|\tau_{t'}))\right]. \end{aligned} \tag{7}$$

Most PPO (Schulman et al., 2017) implementations, both in single-agent and multi-agent environments, use the entropy regularized gradient $\nabla_\theta^\alpha J_{\text{SP}}(\pi_\theta)$. In Yu et al. (2022) it was found that independent PPO (IPPO), and multi-agent PPO (MAPPO), which uses a centralized critic with access to the SAH, instead of a local critic with only access to the local AOH, like IPPO, are effective in learning joint policies with high SP returns in Hanabi and other Dec-POMDPs. In e.g. Muglich et al. (2025) however it was reported that IPPO achieves very low inter-seed XP in Hanabi.

3. Why high enough entropy regularization leads to symmetry equivariance

In this section we assume a tabular softmax parametrization, i.e. for every local AOH τ^i which is possible in the Dec-POMDP, we denote by $\theta^i(a^i|\tau^i)$ the logit corresponding to agent i taking local action a^i given τ^i:

$$\pi^i_\theta(a^i|\tau^i) = \frac{\exp(\theta^i(a^i|\tau^i))}{\sum_{b^i \in \mathcal{A}^i} \exp(\theta^i(b^i|\tau^i))}. \tag{8}$$

We define the space of centered logits

$$\mathbb{R}^d/1 := \left\{ \theta \in \mathbb{R}^d : \forall i, \tau^i : \sum_{a^i \in \mathcal{A}^i} \theta^i(a^i|\tau^i) = 0 \right\}.$$

We let $\theta_0 \in \mathbb{R}^d/1$ be the initial parameters, and set

$$\theta_{k+1} = \theta_k + \beta_k \nabla^\alpha_\theta J_{\mathrm{SP}}(\pi_{\theta_k}), \quad k \in \mathbb{N}_0, \tag{9}$$

for step sizes $\eta_k > 0$, $k \in \mathbb{N}_0$, satisfying the Robbins-Monro conditions $\sum_{k=0}^\infty \eta_k = \infty$, and $\sum_{k=0}^\infty \eta_k^2 < \infty$. When initializing θ_0 randomly and/or using noisy estimates of the gradients, and assuming convergence, there are typically many different limiting policies π_{θ_∞}. Intuitively, increasing the entropy coefficient α "makes the objective function more concave"[1], since entropy is a strictly concave function on the probability simplex, having as its unique maximizer the uniform distribution. For $\alpha \to \infty$, when assuming exact values of $\nabla^\alpha_\theta J_{\mathrm{SP}}(\pi_\theta)$ or unbiased estimates thereof, we can expect the limiting policy π_{θ_∞} to always exist and be the uniformly random policy, for any $\theta_0 \in \mathbb{R}^d/1$. This is because as $\alpha \to \infty$ the relative contribution of the term $\nabla_\theta J_{\mathrm{SP}}(\pi_\theta)$ in $\nabla^\alpha_\theta J_{\mathrm{SP}}(\pi_\theta)$ becomes negligible, and one is just following the vector field $\theta \mapsto \mathbb{E}_{\tau_T \sim \pi_\theta}\left[\nabla_\theta \sum_{t=0}^{T-1} \mathrm{Ent}(\pi_\theta(\cdot|\tau_t))\right]$, which always leads to π_{θ_∞} being the uniformly random policy. We prove the following theorem in Appendix A.

Theorem 3.1. *Let $\theta \mapsto \pi_\theta$ be the tabular softmax parametrization in a Dec-POMDP. Then there exists a finite entropy threshold $\alpha' \in [0, \infty)$, such that for all $\alpha \geq \alpha'$ there exists a unique $\theta_\alpha \in \mathbb{R}^d/1$ at which the vector field $\theta \mapsto \nabla^\alpha_\theta J_{SP}(\pi_\theta)$ equals zero. Furthermore, π_{θ_α} is symmetry equivariant, i.e. $\phi(\pi_{\theta_\alpha}) = \pi_{\theta_\alpha}$ for all $\phi \in \Phi$. Finally, for any θ_0, the sequence (9) almost surely converges to θ_α. This is true both when using the exact gradient $\nabla^\alpha_\theta J_{SP}(\pi_\theta)$, or when using unbiased estimates of $\nabla^\alpha_\theta J_{SP}(\pi_\theta)$ with finite variance, like e.g. REINFORCE-type estimators.*

We emphasize that for α above the entropy threshold, π_{θ_α} might be very close to the uniformly random policy, which means that **the self-play return $J_{\mathrm{SP}}(\pi_{\theta_\alpha})$ might be very low**. However, it is clear that the greedification $\hat{\pi}_{\theta_\alpha}$ is also symmetry equivariant, and $J_{\mathrm{SP}}(\hat{\pi}_{\theta_\alpha})$ might be significantly larger than $J_{\mathrm{SP}}(\pi_{\theta_\alpha})$. We can **find the entropy threshold in practice**, by training a pool of joint policies for each α, until the greedified SP and XP in that pool are equal. For an example of this, see Figure 1.

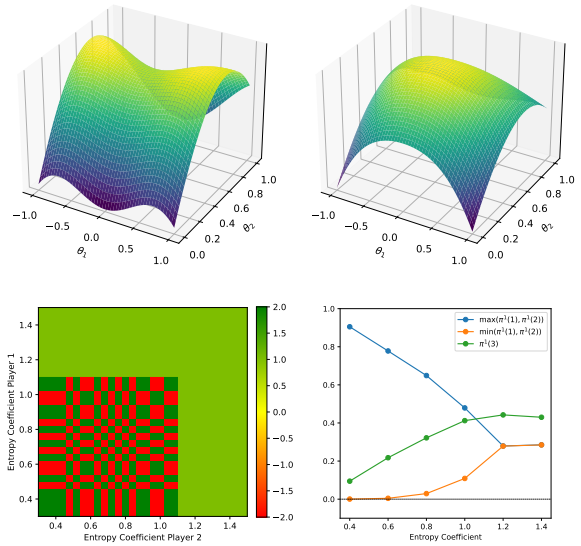

Figure 1. Consider the one-round simultaneous action game with payoff matrix given in (1), and the parametrization $\theta = (\theta_1, \theta_2) \mapsto \mathrm{softmax}(\theta_1, -\theta_1, \theta_2) = \pi^1_\theta(\cdot) = \pi^2_\theta(\cdot)$. **Top**: the function $\theta \mapsto J^\alpha_{\mathrm{SP}}(\pi_\theta)$, with $\alpha = 1.0$ on the left and $\alpha = 1.2$ on the right. **Bottom left**: XP matrix between multiple greedified joint policies, which were trained with entropy regularized independent REINFORCE with baseline, with entropy coefficients 0.4, 0.6, 0.8, 1.0, 1.2, 1.4. 5 seeds per entropy coefficient. **Bottom right**: action probabilities of one trained policy π_θ for each entropy coefficient.

3.1. Why this doesn't work with the maximum entropy RL objective

Theorem 3.1 is easily seen to be true in one-round Dec-POMDPs, i.e. when $T = 1$, since then $\nabla^\alpha_\theta J_{\mathrm{SP}}(\pi_\theta) = \nabla_\theta J^\alpha_{\mathrm{SP}}(\pi_\theta)$ for all $\theta \in \mathbb{R}^d$, implying that then one is maximizing the actual objective function $\pi \mapsto J^\alpha_{\mathrm{SP}}(\pi)$, which becomes strictly concave for large enough α, and for which it is easily seen that $J^\alpha_{\mathrm{SP}}(\phi(\pi)) = J^\alpha_{\mathrm{SP}}(\pi)$ for all $\phi \in \Phi$. For an example of this phenomenon in a simple one-round Dec-POMDP, see Figure 1.

In general Dec-POMDPs however, when using $\nabla_\theta J^\alpha_{\mathrm{SP}}(\pi_\theta)$ instead of $\nabla^\alpha_\theta J_{\mathrm{SP}}(\pi_\theta)$, one can **not** guarantee that for large α the limiting policies will be the same for every initialization θ_0. This is because when there are 2 or more agents, the function $\pi \mapsto \mathbb{E}_{\tau_T \sim \pi}\left[\sum_{t=0}^{T-1} \mathrm{Ent}(\pi(\cdot|\tau_t))\right]$ can have multiple global maxima, and is thus in particular not necessarily concave. For an example, consider a modified version of the

[1] We used quotation marks here to emphasize that in general (see Section 2.4) there isn't actually an objective function whose gradient is given by the vector field $\theta \mapsto \nabla^\alpha_\theta J_{\mathrm{SP}}(\pi_\theta)$.

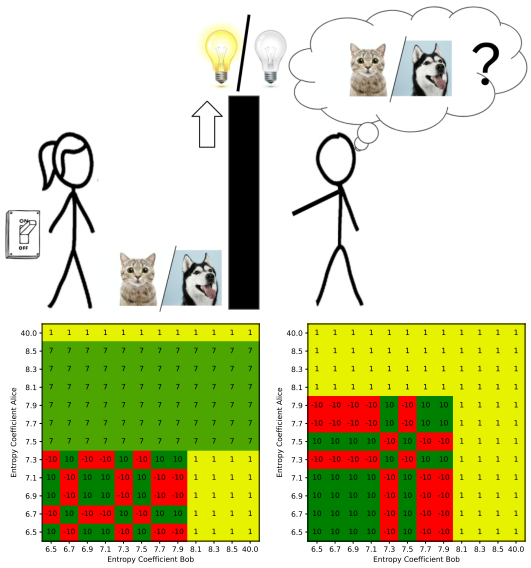

Figure 2. **Top**: Toy cooperative communication game (figure taken from (Hu et al., 2021), with kind permission of the authors): Alice observes the pet and can either signal "on", signal "off", "reveal" for a reward of -3, so that Bob can see the pet, or "bail" out for a reward of 1. Bob then can guess "cat" or "dog" for a reward of ± 10 depending on whether he was correct, or he can "bail" out for a reward of 1. **Bottom left**: XP matrix between greedified policies in the cat/dog game, which are trained with entropy regularized independent REINFORCE with baseline, with different entropy coefficients. **Bottom right**: same as left, except that the reward for "reveal" is now -8 instead of -3.

one-round game with payoff matrix (1), where if the reward in the first round is 2, then there is an additional round where both agents can choose between 10 dummy actions which all give a reward of 0. Then there are two different policies which both maximize $\mathbb{E}_{\tau_T \sim \pi}\left[\sum_{t=0}^{T-1} \text{Ent}(\pi(\cdot|\tau_t))\right]$, namely one under which both agents mostly choose the first action, and one where both mostly choose the second action. Thus using $\nabla_\theta J^\alpha_{\text{SP}}(\pi_\theta)$ and increasing α in this game will *increase* the incentive to break the symmetry.

3.2. An illustrative toy example

Consider the cat/dog toy game from Hu et al. (2021), shown on the top in Figure 2. In this game there are two joint policies which maximize J_{SP}, with a return of 10: one in which Alice always signals "on" when she sees a cat and "off" when she sees a dog, and one in which this pairing is opposite. The XP return of those two joint policies is -10 though. Under the optimal symmetry equivariant joint policy Alice always reveals and Bob then guesses the correct pet, which has a return of 7. There is also a suboptimal symmetry equivariant policy under which Alice always bails, for a return of 1.

On the bottom left in Figure 2 is shown the XP matrix between multiple joint policies trained with different entropy coefficients. We see that for $\alpha \in \{8.1, 8.3, 8.5\}$, both Alice and Bob learn to assign the highest probability to the optimal symmetry equivariant actions. However, we also see that for $\alpha \in \{7.5, 7.7, 7.9\}$, Alice assigns the highest probability to revealing, but that when Bob sees "on" or "off" he breaks the symmetry and guesses a pet instead of bailing, implying that Alice also breaks the symmetry among her suboptimal actions "on" and "off." This means that one does not necessarily need to increase α to the point where the non-greedy policies are symmetry equivariant, but only to the point where the greedfied policies are symmetry equivariant.

3.3. First limitation: Coordination might be impossible above the entropy threshold

Consider a version of the cat/dog game where the reward for revealing the pet is -8 instead of -3. This gives the optimal symmetry equivariant policy a return of 2. The XP matrix for policies trained with different entropy coefficient is shown on the right in Figure 2. In this game, we see that above the threshold for the entropy coefficient where the greedified policies stop breaking symmetries, Alice already prefers bailing over revealing, since she cannot rely on Bob to often enough choose the correct pet when she pays the high cost of revealing. Thus in this game there is no entropy coefficient for which Alice learns to assign revealing the highest probability. We note that the OP (Hu et al., 2020) and OBL (Hu et al., 2021) algorithms are able to learn the optimal symmetry equivariant policy in this game.

The two different version of the cat/dog game provide the intuition that in Dec-POMDPs where there isn't a lot of incentive to break symmetries, i.e. when the return of the optimal symmetry equivariant policy is almost as high as the return of the overall optimal policies, then one can find the optimal symmetry equivariant policy with policy gradient methods, high enough entropy regularization, and subsequent greedification. In games where there are symmetry breaking policies with a much higher return than that of all symmetry equivariant policies, one can still learn symmetry equivariant policies through increasing the entropy coefficient, but (the greedification of) those policies might be highly suboptimal among the symmetry equivariant policies.

3.4. Second limitation: No exploitation of symmetries

For an example of a Dec-POMDP in which one cannot learn the optimal symmetry equivariant policy through sufficiently high entropy regularization, consider the one-round simultaneous action game with payoff matrix

$$\begin{bmatrix} 3 & 0 & 0 \\ 0 & 3 & 0 \\ 0 & 0 & 2 \end{bmatrix}. \tag{10}$$

For high enough α, the local policies of the unique π_{θ_α} will assign equal probability to the first two actions, and a lower probability to the third one. The greedified version of this policy will have a return of 1.5, while the optimal symmetry equivariant policy, under which both local policies always choose the third action, has a return of 2. Intuitively speaking this means that a high entropy coefficient will ensure that the learned policies do not break the symmetries of the Dec-POMDP, but they cannot *exploit* the symmetries either.

4. Experimental Results

We run experiments in the JaxMARL (Rutherford et al., 2024) implementations of the popular Hanabi (Bard et al., 2020) and Overcooked (Carroll et al., 2019) environments, as well as the recently developed Yokai environment (Ruhdorfer et al., 2025), to which we have been kindly given early access by its authors. The hyperparameters that are constant across all our experiments are shown in Appendix B. We will open-source all the code which generated our experimental results in a future version of this paper.

Finding the entropy threshold: We first investigate the entropy thresholds of Hanabi, Overcooked and Yokai, by measuring, for different α, the greedy and non-greedy SP and XP of multiple joint policies trained with IPPO. Those results are shown in Figure 3. Note that for any joint policy in the entire experiments section, $J_{\text{SP}}(\pi)$ is computed as the average over 5000 games.

As expected we see in all environments that as α increases the non-greedy SP and the non-greedy XP eventually meet, but that they decrease for high α. We also see that greedy SP and XP eventually meet, and that, in all environments except Yokai, they are significantly higher than non-greedy SP and XP when α is high. In Yokai the gap between SP and XP is closed only when α is so high that the policies cannot effectively learn anymore. While there might be other hyperparameters that achieve higher XP, our results suggest that the entropy threshold for Yokai is so high that above it no coordination between the local policies is possible anymore.

XP between different entropy coefficients: For 2-player Hanabi and Overcooked we also measure the XP between policies coming from different α. For Hanabi we use 4 different network architectures. The first architecture, referred to as "LSTM", consists of one feed-forward embedding layer, two LSTM layers, and then one actor and one critic head The second architecture, which we refer to as "FF", replaces the two LSTM layers in the LSTM architure by two feedforward layers. Third and fourth, the public-private LSTM architecture described in Figure 5 in the appendix, where the critic is either local or centralized. In the case of a centralized critic, the policy gradient algorithm becomes

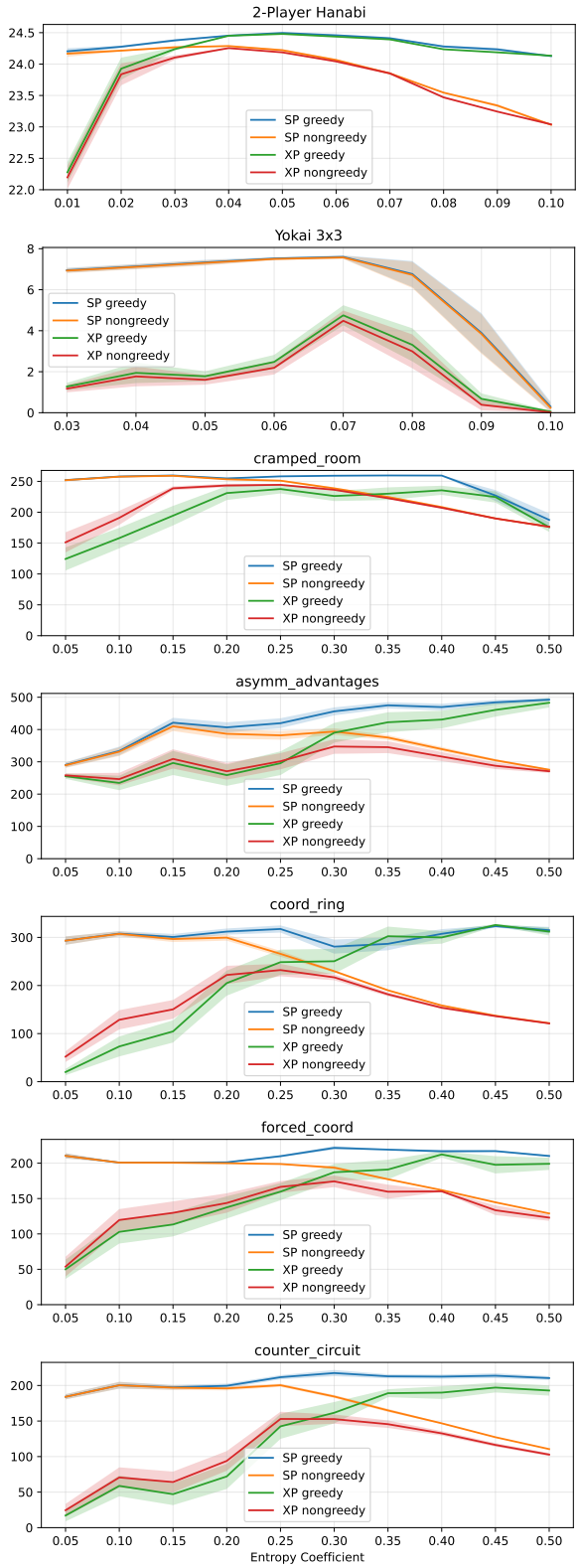

Figure 3. 2-Player Hanabi, 3x3 Yokai, and the five standard Overcooked layouts: Mean SP and XP, greedy and non-greedy, of IPPO with different entropy coefficients α. The shaded regions show one standard error of the mean. We used $\lambda_{\text{GAE}} = 0.9, 0.85, 0.8$, and 4, 16, 48 seeds per α, for Hanabi, Yokai, Overcooked, respectively.

MAPPO (Yu et al., 2022). We use the public-private LSTM architecture in order for the actor architecture to be exactly the same as the one that is used for Off-Belief Learning (OBL) (Hu et al., 2021; Cui et al., 2022). Note that in Figure 3 we used the LSTM architecture for Hanabi.

In 2-player Hanabi, we train four seeds of IPPO policies per αs, for each of the first three architectures. For each of the three architectures we this way obtain 40 joint policies $\pi_1, ..., \pi_{40}$, and compute their greedy XP matrix. These XP matrices are shown in Figures 6, 7, and 8 in the appendix. When taking the average SP and XP in the diagonal 4×4 blocks (same α), and the average XP in the off-diagonal blocks (different α), we get the block XP matrices shown in Figure 4. The corresponding results for Overcooked, when using 10 seeds per α and 10×10 blocks, are shown in Appendix D. As in Figure 3 we see that as α increases the average greedy XP approaches the average greedy SP. But we also see that for sufficiently high α, the policies coming from different α are almost perfectly compatible with each other. We furthermore see that the FF policies are much more likely to break symmetries since they are much worse in XP than the RNN based policies. This can be interpreted as meaning that FF policies struggle to understand what information their partner wants to convey, since they only remember their last observation and their partner's last action. Thus they must rely on very specialized conventions in order to communicate through this bottleneck.

Hanabi: New SOTA in inter-seed XP: The highest XP for the two LSTM architectures in Figure 4 is achieved with $\alpha = 0.05$. In order to avoid a maximization bias, we ran new sets of 4 seeds with $\alpha = 0.05$, for IPPO with the LSTM architecture, and for IPPO and MAPPO with the PP LSTM architecture. We also implemented our own IPPO-based version of OBL and computed again 4 seeds each up to level 6 and level 4 for 2- and 3-player Hanabi, respectively. The average SP and XP are shown in Table 1. We can see that for 2 players, the average XP of IPPO, IPPO PP, and MAPPO PP is significantly higher than our OBL level 6 and the previous SOTA of 24.30 ± 0.01, achieved in Cui et al. (2022). In 3-player Hanabi we also used $\alpha = 0.05$ and see again that the average XP of IPPO, IPPO PP, and MAPPO PP is significantly higher than our OBL level 4 and the previous SOTA of XP in 3-player Hanabi of 23.02 ± 0.01, achieved in Hu et al. (2021). In 4- and 5-player Hanabi, for which to our knowledge no XP returns have been published previously, we used $\alpha = 0.05, 0.08$, respectively. For 5-player Hanabi we computed 5 seeds instead of 4, in order for every local policy in the joint policies formed in XP to come from a different seed. The mean XP and the standard error are computed as the mean and standard error over J_{SP} of all joint policies in which no two local policies come from the same random seed.

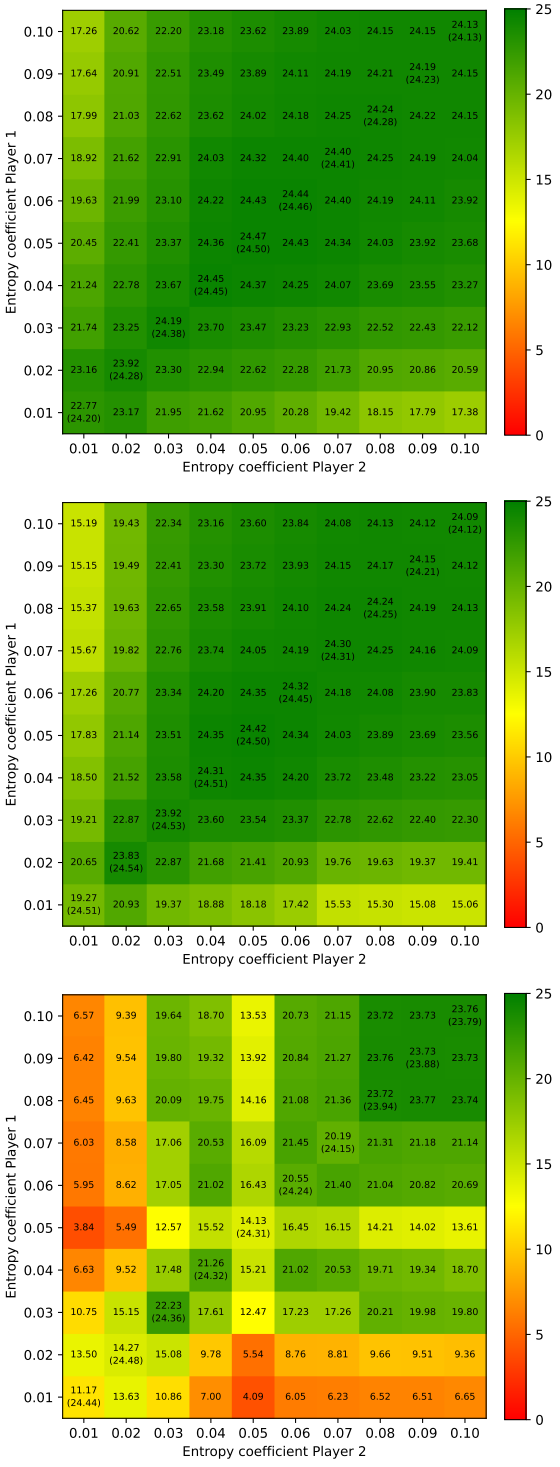

Figure 4. 2-Player Hanabi: Block XP matrices between 40 greedified policies trained with IPPO with different architectures, αs and $\lambda_{\text{GAE}} = 0.9$. Four seeds per α. On the diagonal, the numbers are the average SP (in parentheses) and the average XP in the diagonal 4x4 blocks. The off-diagonal numbers give the average XP in the off-diagonal 4x4 blocks. **Top**: LSTM. **Middle**: PP LSTM. **Bottom**: FF. For the full XP matrices see Figures 6, 7, and 8 in the appendix.

Table 1. Hanabi: Mean ± standard error, for greedy SP and XP, for 4 seeds each of IPPO with LSTM architecture, IPPO with public-private LSTM architecture, MAPPO with public-private LSTM architecture. We use $\lambda_{\text{GAE}} = 0.9$ and $\alpha = 0.05$. In 5-player Hanabi we use $\alpha = 0.08$ and 5 seeds. Also included are scores from our own implementation of OBL (4 seeds per level), as well as for OT-OBL L5 from Cui et al. (2022) (where only XP is explicitly reported) and for OBL L4 from the original OBL paper Hu et al. (2021).

	SP	XP
2P: IPPO $\alpha = 0.05$	24.48 ± 0.02	24.45 ± 0.02
IPPO PP $\alpha = 0.05$	**24.49** ± 0.02	24.46 ± 0.02
MAPPO PP $\alpha = 0.05$	**24.49** ± 0.02	**24.47** ± 0.02
OBL L5 (ours)	24.35 ± 0.02	24.30 ± 0.02
OBL L6 (ours)	24.35 ± 0.02	24.30 ± 0.02
OBL L4 (original)	24.10 ± 0.01	23.76 ± 0.06
OT-OBL L5	-	24.30 ± 0.01
3P: IPPO $\alpha = 0.05$	24.48 ± 0.02	24.28 ± 0.03
IPPO PP $\alpha = 0.05$	**24.66** ± 0.02	**24.55** ± 0.03
MAPPO PP $\alpha = 0.05$	**24.66** ± 0.01	24.54 ± 0.02
OBL L3 (ours)	24.37 ± 0.02	24.34 ± 0.02
OBL L4 (ours)	24.48 ± 0.01	24.47 ± 0.02
OBL L4 (original)	23.38 ± 0.04	23.02 ± 0.01
4P: IPPO $\alpha = 0.05$	24.34 ± 0.09	24.10 ± 0.03
IPPO PP $\alpha = 0.05$	24.55 ± 0.01	**24.30** ± 0.03
MAPPO PP $\alpha = 0.05$	**24.57** ± 0.03	24.24 ± 0.04
5P: IPPO $\alpha = 0.08$	23.32 ± 0.35	21.27 ± 0.12
IPPO PP $\alpha = 0.08$	**23.73** ± 0.02	**23.59** ± 0.03
MAPPO PP $\alpha = 0.08$	23.66 ± 0.21	23.21 ± 0.06

4.1. Hanabi: Biased advantage estimates lead to symmetry breaking

When using a critic in IPPO to reduce the variance in the advantage estimates, we are introducing bias into the estimates of $\nabla^{\alpha}_{\theta} J_{\text{SP}}$, since the critic will not be fully accurate. This bias can also lead to symmetry breaking, since an asymmetrically biased critic will lead the actor to break symmetries. To investigate the effect of asymmetric bias of the critic, we ran IPPO with $\alpha = 0.01, 0.05, 0.10$, and different λ_{GAE}, see Table 2. Note that for all results in the previous sections we used $\lambda_{\text{GAE}} = 0.9$. We see that when λ_{GAE} is too small, i.e. when the generalized advantage estimates heavily rely on the critic and thus have low variance but high bias, then this results in a gap between SP and XP. When λ_{GAE} is too large though, then this can lead to both SP and XP decreasing.

5. Related Work

In Rudolph et al. (2026) it was found that in various imperfect information two-player zero-sum games, generic IPPO with increased entropy regularization beats, in terms of exploitability of the trained policies, other popular algorithms which were specifically designed for this setting.

Table 2. 2-Player Hanabi: Mean ± standard error, of SP and XP of IPPO LSTM policies trained with different entropy coefficients α and λ_{GAE}. 4 seeds per set of hyperparameters.

α	λ_{GAE}	SP	XP
0.01	0.00	22.75 ± 0.41	18.04 ± 1.01
0.01	0.50	**24.43** ± 0.08	5.580 ± 8.08
0.01	0.80	24.41 ± 0.07	14.36 ± 6.45
0.01	0.90	24.18 ± 0.10	22.78 ± 0.79
0.01	0.95	24.16 ± 0.01	22.59 ± 1.00
0.01	1.00	23.52 ± 0.08	**23.14** ± 0.25
0.05	0.00	22.45 ± 0.20	20.09 ± 1.42
0.05	0.50	24.43 ± 0.03	7.940 ± 9.60
0.05	0.80	**24.51** ± 0.01	16.18 ± 7.37
0.05	0.90	24.47 ± 0.01	**24.48** ± 0.02
0.05	0.95	24.31 ± 0.03	24.23 ± 0.08
0.05	1.00	14.96 ± 0.01	14.96 ± 0.01
0.10	0.00	22.12 ± 0.17	20.99 ± 1.03
0.10	0.50	24.16 ± 0.19	22.13 ± 2.08
0.10	0.80	**24.35** ± 0.02	**24.32** ± 0.03
0.10	0.90	24.14 ± 0.02	24.13 ± 0.02
0.10	0.95	14.99 ± 0.01	14.99 ± 0.01
0.10	1.00	10.07 ± 0.02	10.07 ± 0.01

In the concurrent work Lauffer et al. (2025), a new multi-agent policy gradient method called *rational policy gradient* is developed for Dec-POMDPs, which aims to learn policies that are robust and diverse. They also briefly mention that in their experiments in the reduced 3- and 4-color versions of 2-player Hanabi, IPPO with $\alpha = 0.05$ led to higher inter-seed XP than with $\alpha = 0.01$. They speculate that this is a feature of the smaller game or due to the fact that they use feedforward policies without history dependence, but do not expand on it further. Our results show though that higher entropy regularization leading to XP approaching SP is a general phenomenon in Dec-POMDPs, and perfectly closes the gap between SP and XP in full Hanabi with 2, 3, 4, 5 players, and that in fact, policies which lack history dependence, are *more* likely to break symmetries than policies which use RNNs.

6. Conclusion

Through both theoretical and empirical results we have shown that higher entropy regularization during training and greedification after training can be very effective in learning high performing symmetry equivariant policies in Dec-POMDPs, and that this can have a massive influence on inter-seed XP. While we have also demonstrated clear limitations of this recipe, our results indicate that for hyperparameter sweeps in Dec-POMDPs one should sweep over a far bigger range of entropy coefficients than is typically done.

References

Bard, N., Foerster, J. N., Chandar, S., Burch, N., Lanctot, M., Song, H. F., Parisotto, E., Dumoulin, V., Moitra, S., Hughes, E., et al. The Hanabi Challenge: A New Frontier for AI Research. *Artificial Intelligence*, 280: 103216, 2020.

Borkar, V. S. *Stochastic Approximation: A Dynamical Systems Viewpoint. Second edition.* New Delhi: Hindustan Book Agency, 2023.

Carroll, M., Shah, R., Ho, M. K., Griffiths, T., Seshia, S., Abbeel, P., and Dragan, A. On the Utility of Learning about Humans for Human-AI Coordination. *Advances in Neural Information Processing Systems*, 2019.

Cui, B., Hu, H., Pineda, L., and Foerster, J. K-level Reasoning for Zero-Shot Coordination in Hanabi. *Advances in Neural Information Processing Systems*, 2021.

Cui, B., Hu, H., Lupu, A., Sokota, S., and Foerster, J. Off-team learning. *Advances in Neural Information Processing Systems*, 2022.

Dizdarević, T., Hammond, R., Gessler, T., Calinescu, A., Cook, J., Gallici, M., Lupu, A., and Foerster, J. Ad-Hoc Human-AI Coordination Challenge. *International Conference on Machine Learning*, 2025.

Gessler, T., Dizdarevic, T., Calinescu, A., Ellis, B., Lupu, A., and Foerster, J. OvercookedV2: Rethinking Overcooked for Zero-Shot Coordination. *International Conference on Learning Representations*, 2025.

Hu, H., Lerer, A., Peysakhovich, A., and Foerster, J. "Other-Play" for Zero-Shot Coordination. *International Conference on Machine Learning*, 2020.

Hu, H., Lerer, A., Cui, B., Pineda, L., Brown, N., and Foerster, J. Off-Belief Learning. *International Conference on Machine Learning*, 2021.

Lauffer, N., Shah, A., Carroll, M., Seshia, S. A., Russell, S., and Dennis, M. Robust and diverse multi-agent learning via rational policy gradient. *Advances in Neural Information Processing Systems*, 2025.

Lupu, A., Cui, B., Hu, H., and Foerster, J. Trajectory Diversity for Zero-Shot Coordination. *International Conference on Machine Learning*, 2021.

Muglich, D., Schroeder de Witt, C., van der Pol, E., Whiteson, S., and Foerster, J. Equivariant Networks for Zero-Shot Coordination. *Advances in Neural Information Processing Systems*, 2022.

Muglich, D., Forkel, J., van der Pol, E., and Foerster, J. Expected return symmetries. *International Conference on Learning Representations*, 2025.

Oliehoek, F. A., Spaan, M. T., Vlassis, N., et al. Dec-POMDPs with delayed communication. *The 2nd Workshop on Multi-agent Sequential Decision-Making in Uncertain Domains*, 2007.

Rudolph, M., Lichtle, N., Mohammadpour, S., Bayen, A., Kolter, J. Z., Zhang, A., Farina, G., Vinitsky, E., and Sokota, S. Reevaluating Policy Gradient Methods for Imperfect-Information Games. *International Conference on Learning Representations*, 2026.

Ruhdorfer, C., Bortoletto, M., and Bulling, A. The Yokai Learning Environment: Tracking Beliefs Over Space and Time, 2025. URL https://arxiv.org/abs/2508.12480.

Rutherford, A., Ellis, B., Gallici, M., Cook, J., Lupu, A., Ingvarsson, G., Willi, T., Hammond, R., Khan, A., de Witt, C. S., Souly, A., Bandyopadhyay, S., Samvelyan, M., Jiang, M., Lange, R. T., Whiteson, S., Lacerda, B., Hawes, N., Rocktaschel, T., Lu, C., and Foerster, J. N. Jaxmarl: Multi-agent rl environments and algorithms in jax, 2024. URL https://arxiv.org/abs/2311.10090.

Schulman, J., Wolski, F., Dhariwal, P., Radford, A., and Klimov, O. Proximal policy optimization algorithms, 2017. URL https://arxiv.org/abs/1707.06347.

Treutlein, J., Dennis, M., Oesterheld, C., and Foerster, J. A New Formalism, Method and Open Issues for Zero-Shot Coordination. *International Conference on Machine Learning*, 2021.

Yu, C., Velu, A., Vinitsky, E., Gao, J., Wang, Y., Bayen, A., and Wu, Y. The Surprising Effectiveness of PPO in Cooperative, Multi-Agent Games. *Advances in Neural Information Processing Systems*, 2022.

A. Proof of Theorem 3.1

In order to prove Theorem 3.1, we need the following classical result on stochastic approximation:

Theorem A.1 (Theorem 2.1, Corollary 2.2, Theorem 4.4 in (Borkar, 2023))**.** *Given a (possible random) $\theta_0 \in \mathbb{R}^d$, consider the stochastic process $(\theta_k, k \in \mathbb{N}_0)$ in $\mathbb{R}^d$, defined by the recursion*

$$\theta_{k+1} = \theta_k + \eta_k(F(\theta_k) + M_{k+1}), \quad k \in \mathbb{N}_0, \tag{11}$$

where:

1. *$F : \mathbb{R}^d \to \mathbb{R}^d$ is Lipschitz with a unique zero $\theta_* \in \mathbb{R}^d$. Furthermore, for any $\hat{\theta}_0 \in \mathbb{R}^d$ it holds that $\lim_{t\to\infty} \hat{\theta}_t = \hat{\theta}_*$, where $t \mapsto \hat{\theta}_t$ satisfies the ODE $\frac{d\hat{\theta}_t}{dt} = F(\hat{\theta}_t)$.*
2. *The step sizes $\eta_k > 0$, $k \in \mathbb{N}_0$ satisfy $\sum_{k=0}^{\infty} \eta_k = \infty$ and $\sum_{k=0}^{\infty} \eta_k^2 < \infty$.*
3. *$(M_k, k \in \mathbb{N})$ is a martingale difference sequence w.r.t the increasing family of σ-algebras*

$$\mathcal{F}_k := \sigma(\theta_l, M_l, \leq l \leq k) = \sigma(\theta_0, M_1, ..., M_k), \tag{12}$$

   i.e. $\mathbb{E}[M_{k+1}|\mathcal{F}_k] = 0$ almost surely for all $k \in \mathbb{N}$. Furthermore $\mathbb{E}\left[\|M_k\|^2\right] < \infty$ for all $k \in \mathbb{N}$, and there exists a constant $K > 0$, such that $\mathbb{E}\left[\|M_k\|^2\right] \leq K(1 + \|\theta_k\|^2)$ for all $k \in \mathbb{N}$.
4. *There exists a twice continuously differentiable Lyapunov function $V : \mathbb{R}^d \to \mathbb{R}_{\geq 0}$ which has bounded second derivatives and satisfies:*
   (a) $\lim_{\|\theta\|\to\infty} V(\theta) = \infty$,
   (b) There exists $M > 0$, such that $V(\theta) \geq M \implies \langle \nabla_\theta V(\theta), F(\theta)\rangle < 0$.

Then $\mathbb{P}\left(\lim_{k\to\infty} \theta_k = \theta_*\right) = 1$.

Furthermore, we state and prove the following two auxiliary lemmas.

Lemma A.2. *Let $\theta \in \mathbb{R}^d$ and let $\pi_\theta = softmax(\theta) \in (0,1)^d$. Then $\mathbb{E}_{\pi_\theta}[\theta] \geq \frac{1}{d}\sum_{a=1}^d [\theta(a)]$.*

Proof. Define the function $g(\beta) = \langle \pi_{\beta\theta}, \theta\rangle$ and let $H(\pi_\theta) = \frac{\mathrm{d}\pi_\theta}{\mathrm{d}\theta} = \mathrm{Diag}(\pi_\theta) + \pi_\theta\pi_\theta^T \in \mathbb{R}^{d\times d}$. Then

$$g(0) = \frac{1}{d}\sum_{a=1}^d \theta(a), \quad g(1) = \mathbb{E}_{\pi_\theta}[\theta], \quad \frac{\mathrm{d}g}{\mathrm{d}\beta}(\beta) = \langle \theta, H(\pi_{\beta\theta}\theta\rangle = \mathrm{Var}_{\pi_{\beta\theta}}[\theta] \geq 0, \tag{13}$$

which implies the claim. □

Lemma A.3. *Let $\pi_\theta = softmax(\theta) \in (0,1)^d$ for $\theta \in \mathbb{R}^d$, let $\alpha > 0$, let $x \mapsto r_x \in [-1,1]^d$ be a continuous function, and let $x \mapsto \theta_x$ be the solution to the ODE*

$$\frac{d\theta_x}{dx} = \nabla_\theta\left(\pi_{\theta_x}^T(r_x - \alpha\log\pi_{\theta_x})\right), \ x \geq 0, \tag{14}$$

for a starting point θ_0 which satisfies $\sum_{a=1}^d \theta(a) = 0$. Then for all $\epsilon > 0$ there exists a constant $C > 0$, such that

$$|\theta_x(a)| \geq (d-1)(2+\epsilon)\alpha^{-1} \implies sign(\theta_x(a))\frac{d\theta_x}{dx} \leq -\epsilon C < 0, \tag{15}$$

so in particular there exists $x' \in [0,\infty)$, such that $x \geq x' \implies \|\theta_x\|_\infty \leq (d-1)(2+\epsilon)\alpha^{-1}$.

Proof. We see that

$$\frac{\mathrm{d}\theta_x}{\mathrm{d}x} = \pi_{\theta_x} \odot \left(r_x - \alpha\log\pi_{\theta_x} - \mathbb{E}_{\pi_{\theta_x}}[r_x] + \alpha\mathrm{Ent}(\pi_{\theta_x})\right) \tag{16}$$

$$= \pi_{\theta_x} \odot \left(r_x - \alpha\theta_x - \mathbb{E}_{\pi_{\theta_x}}[r_x - \alpha\theta_x]\right). \tag{17}$$

Thus $\frac{\mathrm{d}}{\mathrm{d}x}\sum_{a=1}^{d}\theta_x(a) = \sum_{a=1}^{d}\frac{\mathrm{d}}{\mathrm{d}x}\theta_x(a) = \mathbb{E}_{\pi_{\theta_x}}[r_x - \alpha\theta_x] - \mathbb{E}_{\pi_{\theta_x}}[r_x - \alpha\theta_x] = 0$ for all $x \geq 0$, which together with the assumption that $\sum_{a=0}^{d}\theta_0(a) = 0$ implies that $\sum_{a=1}^{d}\theta_x(a) = 0$ for all $x \geq 0$. Furthermore, since $r_x \in [-1,1]^d$ and by Lemma A.2 $\sum_{a=1}^{d}\theta(a) = 0 \implies \mathbb{E}_{\pi_\theta}[\theta] \geq 0$, we see that

$$r_x(a) - \alpha\theta_x(a) - \mathbb{E}_{\pi_{\theta_x}}[r_x - \alpha\theta_x] \geq -2 - \alpha\theta_x(a),\ a = 1, ..., d. \tag{18}$$

Thus for any $\epsilon > 0$ we see that

$$-\theta_x(a) \geq (2+\epsilon)\alpha^{-1} \implies \frac{\mathrm{d}\theta_x}{\mathrm{d}x} \geq \epsilon\pi_{\theta_x}(a) > 0, \tag{19}$$

which implies that $\inf_{x\geq 0}\min_a\theta_x(a) \geq \min\{-(2+\epsilon)\alpha^{-1}, \min_a\theta_0(a)\}$. Furthermore, since $\frac{\mathrm{d}}{\mathrm{d}x}\sum_{a=1}^{d}\theta_x(a) = 0$ for all $x \geq 0$, we also see that

$$\theta_x(a) > (d-1)(2+\epsilon)\alpha^{-1} \implies \frac{\mathrm{d}\theta_x}{\mathrm{d}x}(a) \leq -(d-1)\epsilon\pi_{\theta_x}(a) < 0, \tag{20}$$

which implies that $\sup_{x\geq 0}\max_a\theta_x(a) \leq \max\{(d-1)(2+\epsilon)\alpha^{-1}, \max_a\theta_0(a)\}$. Thus we see that $C := \inf_{x\geq 0}\min_a\pi_{\theta_x}(a) > 0$, which implies that

$$|\theta_x(a)| \geq (d-1)(2+\epsilon)\alpha^{-1} \implies \mathrm{sign}(\theta_x(a))\frac{\mathrm{d}\theta_x}{\mathrm{d}x}(a) \leq -\epsilon C < 0. \tag{21}$$

□

We now prove Theorem 3.1, which we state here again for completion.

Theorem A.4. *Let $\theta \mapsto \pi_\theta$ be the tabular softmax parametrization in a Dec-POMDP. Then there exists a finite entropy threshold $\alpha' \in [0,\infty)$, such that for all $\alpha \geq \alpha'$ there exists a unique $\theta_\alpha \in \mathbb{R}^d/1$ at which the vector field $\theta \mapsto \nabla^\alpha_\theta J_{SP}(\pi_\theta)$ equals zero. Furthermore, π_{θ_α} is symmetry equivariant, i.e. $\phi(\pi_{\theta_\alpha}) = \pi_{\theta_\alpha}$ for all $\phi \in \Phi$. Finally, for any θ_0, the sequence (9) almost surely converges to θ_α. This is true both when using the exact gradient $\nabla^\alpha_\theta J_{SP}(\pi_\theta)$, or when using unbiased estimates of $\nabla^\alpha_\theta J_{SP}(\pi_\theta)$ with finite variance, like e.g. REINFORCE-type estimators.*

Proof. We see that

$$\begin{aligned}
\nabla^\alpha_\theta J_{\mathrm{SP}}(\pi_\theta) =& \nabla_\theta J_{\mathrm{SP}}(\pi_\theta) + \alpha\mathbb{E}_{\tau_T\sim\pi_\theta}\left[\nabla_\theta\sum_{t=0}^{T-1}\gamma^t\mathrm{Ent}(\pi_\theta(\cdot|\tau_t))\right] && (22)\\
=& \mathbb{E}_{\tau_T\sim\pi_\theta}\left[\sum_{t=0}^{T-1}\gamma^t\sum_{i=1}^{n}\left(\alpha\nabla_\theta\mathrm{Ent}(\pi^i_\theta(\cdot|\tau^i_t)) + \nabla_\theta\log\pi^i_\theta(a^i_t|\tau^i_t)\sum_{t'=t}^{T-1}\gamma^{t'-t}\mathcal{R}(s_{t'+1}, a_{t'})\right)\right] && (23)\\
=& \sum_{t=0}^{T-1}\gamma^t\sum_{i=1}^{n}\sum_{\tau^i_t}p_{\pi_\theta}(\tau^i_t)\left(\alpha\nabla_\theta\mathrm{Ent}(\pi^i_\theta(\cdot|\tau^i_t)) + \sum_{a^i_t}\nabla_\theta\pi^i_\theta(a^i_t|\tau^i_t)Q^i_{\pi_\theta}(a^i_t|\tau^i_t)\right) && (24)\\
=& \sum_{t=0}^{T-1}\gamma^t\sum_{i=1}^{n}\sum_{\tau^i_t}p_{\pi_\theta}(\tau^i_t)\sum_{a^i_t}\nabla_\theta\pi^i_\theta(a^i_t|\tau^i_t)\left(-\alpha\theta^i(a^i_t|\tau^i_t) + Q^i_{\pi_\theta}(a^i_t|\tau^i_t)\right), && (25)
\end{aligned}$$

where $Q^i_{\pi_\theta}(a^i_t|\tau^i_t) = \mathbb{E}_{\tau_T\sim\pi_\theta}\left[\sum_{t'=t}^{T-1}\gamma^{t'-t}\mathcal{R}(s_{t'+1}, a_{t'})|a^i_t, \tau^i_t\right]$. Define the map

$$G : [0,\infty)\times\mathbb{R}^d/1 \to \mathbb{R}^d/1 = \left\{\theta\in\mathbb{R}^d : \forall i, \tau^i : \sum_{a^i\in\mathcal{A}}\theta^i(a^i|\tau^i) = 0\right\} \tag{26}$$

$$(\epsilon,\theta) \mapsto \epsilon\nabla_\theta J_{\mathrm{SP}}(\pi_\theta) + \mathbb{E}_{\tau_T\sim\pi_\theta}\left[\nabla_\theta\sum_{t=0}^{T-1}\gamma^t\mathrm{Ent}(\pi_\theta(\cdot|\tau_t))\right], \tag{27}$$

which, as a composition of smooth functions, is smooth. We see that $G(0,\theta) \iff \theta = 0$ because for every $\theta \in \mathbb{R}^d/1$ every realizable local AOH τ_t^i happens with positive probability and only for $\theta = 0$ is $\nabla_\theta \text{Ent}(\pi_\theta^i(\cdot|\tau_t^i)) = 0$ for all local AOHs τ_t^i. We now show that the Jacobian w.r.t. θ of G is negative definite for $\epsilon = 0$ and $\theta = 0$, and thus invertible (both statements are to be understood in $\mathbb{R}^d/1$, the space of centered logits):

$$\text{Jac}_\theta G(0,\theta) = \sum_{t=0}^{T-1} \gamma^t \sum_{i=1}^{n} \sum_{\tau_t^i} \left(p_{\pi_\theta}(\tau_t^i) \text{Hess}_\theta \text{Ent}(\pi_\theta^i(\cdot|\tau_t^i)) + \nabla_\theta \text{Ent}(\pi_\theta^i(\cdot|\tau_t^i)) \left(\nabla_\theta p_{\pi_\theta}(\tau_t^i)\right)^T \right). \tag{28}$$

Since for every $\theta \in \mathbb{R}^d/1$ it holds that $p_{\pi_\theta}(\tau_t^i) > 0$ for all τ_t^i, and since for $\theta = 0$ it holds that $\nabla_\theta \text{Ent}(\pi_\theta^i(\cdot|\tau_t^i)) = 0$ for all τ_t^i, we see that $\text{Jac}_\theta G(0,0)$ is negative definite as it is a block-diagonal matrix with negative definite blocks.

Thus by the implicit function theorem, there exist $\epsilon' > 0$ and $R > 0$ such that there exists a unique function $g : [0, \epsilon') \to \{\theta \in \mathbb{R}^d/1 : \|\theta\|_\infty < R\}$ for which $g(0) = 0$ and $G(\epsilon, g(\epsilon)) = 0$ for all $\epsilon \in [0, \epsilon')$. Since $\text{Jac}_\theta G(0,0)$ is negative definite, we can assume w.l.o.g. that ϵ' and R were chosen small enough such that for all $\epsilon \in [0, \epsilon')$ and $\|\theta\|_\infty < R$ it holds that $\langle \theta - g(\epsilon), G(\epsilon, \theta) \rangle < 0$.

We see that for $\alpha > 0$ it holds that $\nabla_\theta^\alpha J_{\text{SP}}(\pi_\theta) = \alpha G(\alpha^{-1}, \theta)$. We choose $\alpha' = (\epsilon')^{-1}$, and for $\alpha > \alpha'$ set $\theta_\alpha = g(\alpha^{-1})$. Then, given that g is unique, we see that when $\alpha > \alpha'$ and $\|\theta\|_\infty < R$, then $\nabla_\theta^\alpha J_{\text{SP}}(\pi_\theta) = 0 \iff \theta = \theta_\alpha$.

We now abuse notation and denote by $\theta_x, x \in \mathbb{R}_{\geq 0}$, the trajectory of the ODE

$$\frac{\text{d}\theta_x}{\text{d}x} = \nabla_\theta^\alpha J_{\text{SP}}(\pi_{\theta_x}), \ x \in \mathbb{R}_{\geq 0}, \tag{29}$$

given an initialization θ_0. We then see that for $\alpha > \alpha'$ and $\|\theta_x\|_\infty < R$ the Lyapunov function $V_\alpha(\theta) := \frac{1}{2}\|\theta - \theta_\alpha\|_2^2$ satisfies

$$\frac{\text{d}}{\text{d}x} V_\alpha(\theta_x) = \langle \theta_x - \theta_\alpha, \frac{\text{d}\theta_x}{\text{d}x} \rangle = \langle \theta_x - \theta_\alpha, \nabla_\theta^\alpha J_{\text{SP}}(\pi_\theta) \rangle = \alpha \langle \theta_x - \theta_\alpha, G(\alpha^{-1}, \theta_x) \rangle < 0. \tag{30}$$

By the Lyapunov stability criterion, this implies that if $\|\theta_x\|_\infty < R$, then $\lim_{x\to\infty} V_\alpha(\theta_x) = 0$ and thus $\lim_{x\to\infty} \theta_x = \theta_\alpha$.

We now further assume w.l.o.g. that α' was chosen such that

$$\alpha' \geq 2R^{-1}(|\mathcal{A}| - 1) \max_{\tau_t^i, a_t^i \in \mathcal{A}^i, \theta \in \mathbb{R}^d} Q_{\pi_\theta}^i(a_t^i|\tau_t^i), \tag{31}$$

where the lower bound on the RHS is finite since the state, action and observation spaces, the rewards, and the time horizon are all finite. Applying Lemma A.3 iteratively for $t = 0, ..., T-1$, implies that for any $\alpha > \alpha'$ and θ_0 there exists $x' \geq 0$, such that for all $x \geq x'$ it holds that $\|\theta_x\|_\infty < R$, which in particular implies that for $\alpha > \alpha'$ and $\|\theta\|_\infty \geq R$ it holds that $\nabla_\theta^\alpha J_{\text{SP}}(\pi_\theta) \neq 0$. Since we have already established that $\lim_{x\to\infty} \theta_x = \theta_\alpha$ if $\|\theta_x\|_\infty < R$ for some $x \geq 0$, we see that for any θ_0 it holds that $\lim_{x\to\infty} \theta_x = \theta_\alpha$.

Lemma A.3 then also implies that for $\alpha > \alpha'$, it holds that

$$\|\theta_x\|_\infty \geq R \implies D^+\|\theta_x\|_\infty = \max_{(i,a^i,\tau^i) \in A(\theta)} \text{sign}(\theta_x(\hat{a}^i|\hat{\tau}^i)) \frac{\text{d}}{\text{d}x} \theta_x^i(\hat{a}^i|\hat{\tau}^i) < 0, \tag{32}$$

where $A(\theta) := \text{argmax}_{i,a^i,\tau^i} |\theta^i(a^i|\tau^i)|$, and where we used the upper Dini derivative D^+ since $\theta \mapsto \|\theta\|_\infty$ isn't differentiable at θ for which $A(\theta)$ contains more than one element. It is now straightforward to construct a smooth Lyapunov function $V : \mathbb{R}^d/1 \to \mathbb{R}_{\geq 0}$, which has bounded second derivatives, which satisfies $\lim_{\|\theta\|_\infty \to \infty} V(\theta) = \infty$, and $\|\theta\|_\infty \geq R \implies \langle \nabla_\theta V(\theta), \nabla_\theta^\alpha J_{\text{SP}}(\pi_\theta) \rangle < 0$. Thus all the conditions of Theorem A.1, are satisfied, which implies that for any θ_0 and $\alpha > \alpha'$ the sequence $\theta_{k+1} = \theta_k + \eta_k \nabla_\theta^\alpha J_{\text{SP}}(\pi_{\theta(k)})$, $k \in \mathbb{N}_0$, converges to θ_α. Since $\theta \mapsto \nabla_\theta^\alpha J_{\text{SP}}(\pi_{\theta(k)})$ is bounded, Theorem A.1 implies that we can also use estimates of it with finite variance and still converge almost surely to θ_α for any θ_0.

We now show that $\phi(\pi_{\theta_\alpha}) = \pi_{\theta_\alpha}$ for all $\phi \in \Phi$. Applying ϕ to a policy π_θ merely corresponds to a permutation of the probabilities, which means we can interpret ϕ also as a $d \times d$ permutation matrix, which by the permutation invariance of the softmax function we can also apply to the logits $\theta \in \mathbb{R}^d$. Thus we can write $\phi(\pi_\theta) = \pi_{\phi(\theta)}$. If we can show that $\phi(\nabla_\theta^\alpha J_{\text{SP}}(\pi_\theta)) = \nabla_\theta^\alpha J_{\text{SP}}(\pi_{\phi(\theta)})$ for all $\theta \in \mathbb{R}^d$, then we see that

$$0 = \nabla_\theta^\alpha J_{\text{SP}}(\pi_{\theta_\alpha}) \implies \phi(0) = \phi(\nabla_\theta^\alpha J_{\text{SP}}(\pi_{\theta_\alpha})) \implies 0 = \nabla_\theta^\alpha J_{\text{SP}}(\pi_{\phi(\theta_\alpha)}) \implies \phi(\theta_\alpha) = \theta_\alpha. \tag{33}$$

From the definition of Dec-POMDP symmetries it is fairly straightforward to see that $J_{\text{SP}}(\phi(\pi_\theta)) = J_{\text{SP}}(\pi_\theta)$. This was rigorously proven in Treutlein et al. (2021). Thus by the chain rule and the fact that the inverse of a permutation matrix is given by its transpose, we see that $\nabla_\theta J_{\text{SP}}(\pi_\theta) = \nabla_\theta (J_{\text{SP}} \circ \phi)(\pi_\theta) = \phi^{-1} \left(\nabla_\theta J_{\text{SP}}\right)(\phi(\pi_\theta))$. By similarly straightforward arguments one can verify the intuitive fact that $\phi(G(0, \theta)) = G(0, \phi(\theta))$ for all $\theta \in \mathbb{R}^d$ and $\phi \in \Phi$. This finishes the proof.

□

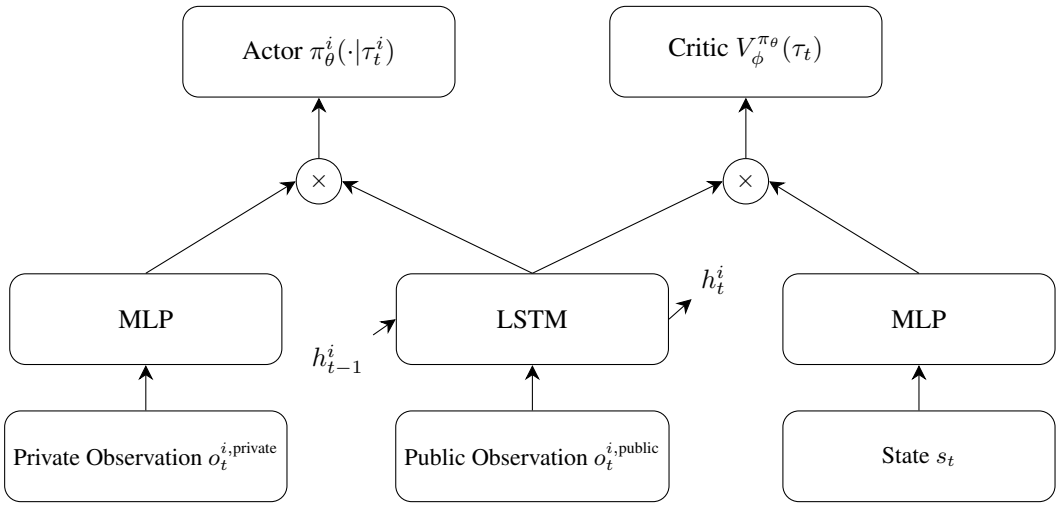

Figure 5. Public-Private LSTM Actor-Critic Architecture: In Hanabi, a player's public observation includes everything except for the player hands. A player's private observation is the public observation plus the other players' hands. The state is the public observation plus all players' hands. For IPPO one technically doesn't need a separate MLP for the critic, as the critic conditions only the local AOH τ_t^i, just like the actor, but we still use a critic MLP which just receives the private observation $o_t^{i,\text{private}}$ as well. Both MLP streams have 3 hidden layers, and the LSTM stream has one feedforward embedding layer and two LSTM layers.

B. Hyperparameters

B.1. Hanabi

In all architectures we use a width of 512 in all layers. All non-LSTM layers have a ReLU activation. For a description of the public-private LSTM architecture see Figure 5. Furthermore we share weights between all agents.

For the PPO hyperparameters that are constant across all our Hanabi experiments, see Table 3 below. The only non-standard implementation detail in our code is that we mask out the actor loss and the entropy bonus for the non-acting player, as it always contributes zero to the gradient. This prevents the actor loss and the entropy bonus from effectively being divided by the number of agents and allows for more consistent hyperparameters across 2, 3, 4, and 5 player Hanabi.

To train our OBL agents, we used 10^{10} total timesteps to train level 1, and 5×10^9 to train all subsequent levels, where we starting training of level k with the final weights from level $k-1$. The architecture of the belief model is exactly the same as the one used in Hu et al. (2021), and is trained through supervised learning.

Table 3. PPO hyperparameters that are fixed across all our Hanabi experiments.

Hyperparameter	**Value**
Learning Rate	5×10^{-4}
Number of Environments	1024
Number of Steps per Rollout	128
Total Timesteps	10^{10}
Update Epochs	4
Number of Minibatches	4
Discount Factor (γ)	0.999
Clipping Coefficient	0.2
Value Function Coefficient	0.5
Max Gradient Norm	0.5
Linear Learning Rate Annealing	True
Optimizer	Adam
Initialization	Orthogonal

B.2. Overcooked

Our actor-critic network for Overcooked is shared between both agents and has the following architecture: the observations are embedded through 3 CNN layers with 32 features each, and kernel sizes of $(5, 5)$, $(3, 3)$, $(3, 3)$, with ReLU activations in between, followed by a fully connected layer with output dimension 64. This embedding is them concatenated with a one-layer fully connected embedding of the environment timestep t. This concatenation is fed through two further fully connected layers with output dimension 64 and ReLU activation, after which there are separate actor and critic heads. We gave the environment timestep to the actor-critic network since otherwise the input isn't Markov as the agents cannot tell when the game ends. The PPO hyperparameters are given in Table 4

Table 4. PPO hyperparameters that are fixed across all our Overcooked experiments.

Hyperparameter	**Value**
Learning Rate	4×10^{-4}
Number of Environments	64
Number of Steps per Rollout	256
Total Timesteps	10^8
Reward Shaping Timesteps	5×10^7
Update Epochs	4
Number of Minibatches	16
Discount Factor (γ)	0.99
λ_{GAE}	0.8
Clipping Coefficient	0.2
Value Function Coefficient	0.5
Max Gradient Norm	0.5
Linear Learning Rate Annealing	True
Optimizer	Adam
Initialization	Orthogonal

B.3. Yokai

Our actor-critic network for Yokai and our chosen hyperparameters are adapted from Ruhdorfer et al. (2025). Specifically, we use their best-performing CNN encoder which uses 4 CNN layers with 64 filters, kernel size $(3, 3)$ and ReLU activation each. The stride is 1 and we employ valid padding. The resulting embedding is fed to a linear projection (to project the CNN output to the GRU hidden size), followed by a GRU and the actor and critic heads respectively. The hidden dimension of the dense layer and the GRU is 256. All hyperparameters are shown in Table 5.

All our experiments were conducted in the 3x3 version of Yokai with memory help tuned on. This corresponds to the ZSC experimental setting in the original paper. For all environment details, we refer the reader to the original work (Ruhdorfer et al., 2025).

Table 5. PPO hyperparameters that are fixed across all our Yokai experiments.

Hyperparameter	**Value**
Learning Rate	3×10^{-4}
Number of Environments	1024
Number of Steps per Rollout	128
Total Timesteps	10^9
Reward Shaping Timesteps	10^9 (linearly annealed)
Update Epochs	4
Number of Minibatches	4
Discount Factor (γ)	0.99
λ_{GAE}	0.85
Clipping Coefficient	0.2
Value Function Coefficient	0.5
Max Gradient Norm	0.5
Linear Learning Rate Annealing	True
Optimizer	Adam
Initialization	Orthogonal

C. Full XP Matrices in Hanabi

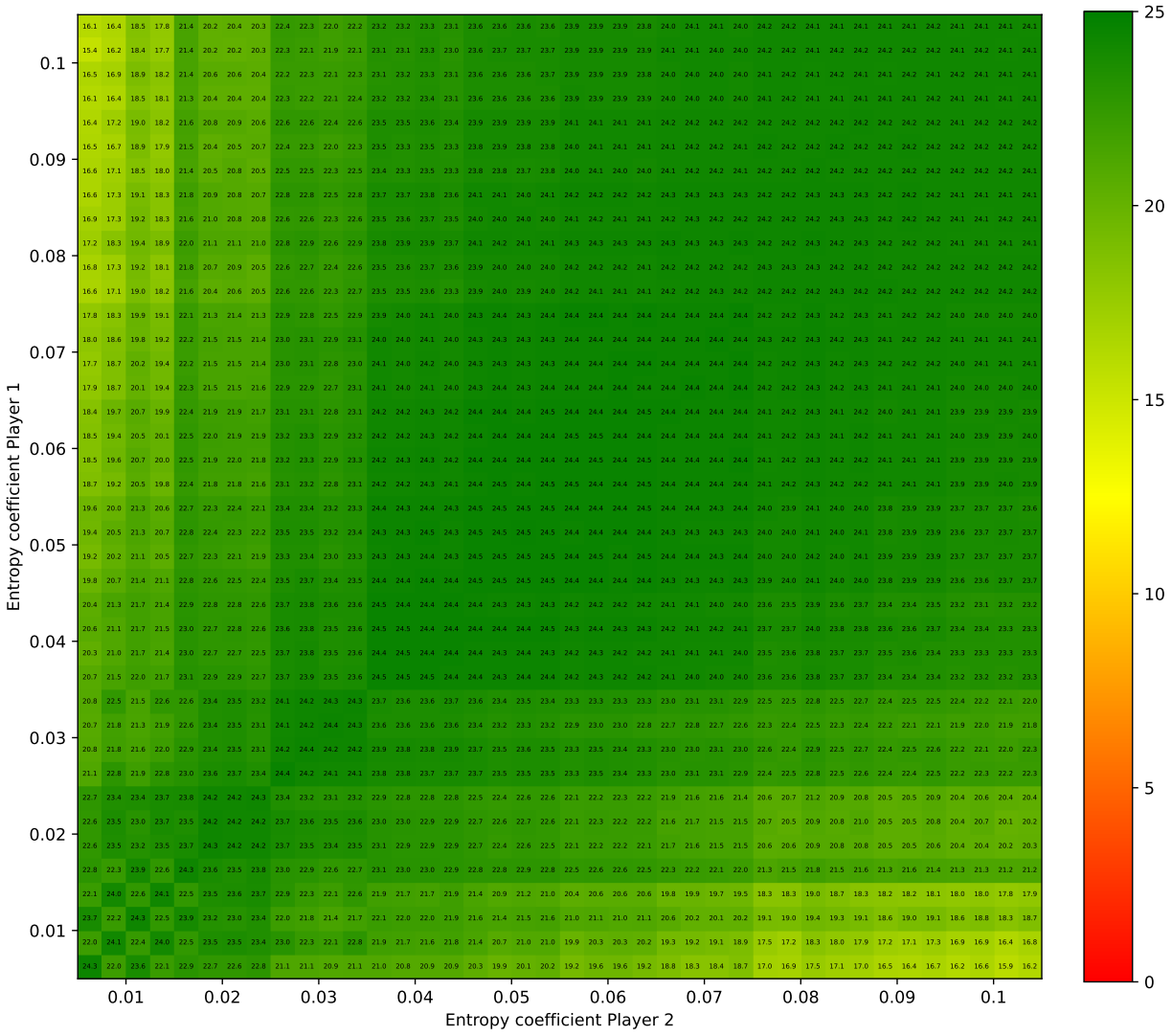

Figure 6. 2-Player Hanabi: XP matrix between LSTM IPPO policies trained with different entropy coefficients. Four seeds per entropy coefficient $0.01, 0.02, ..., 0.10$.

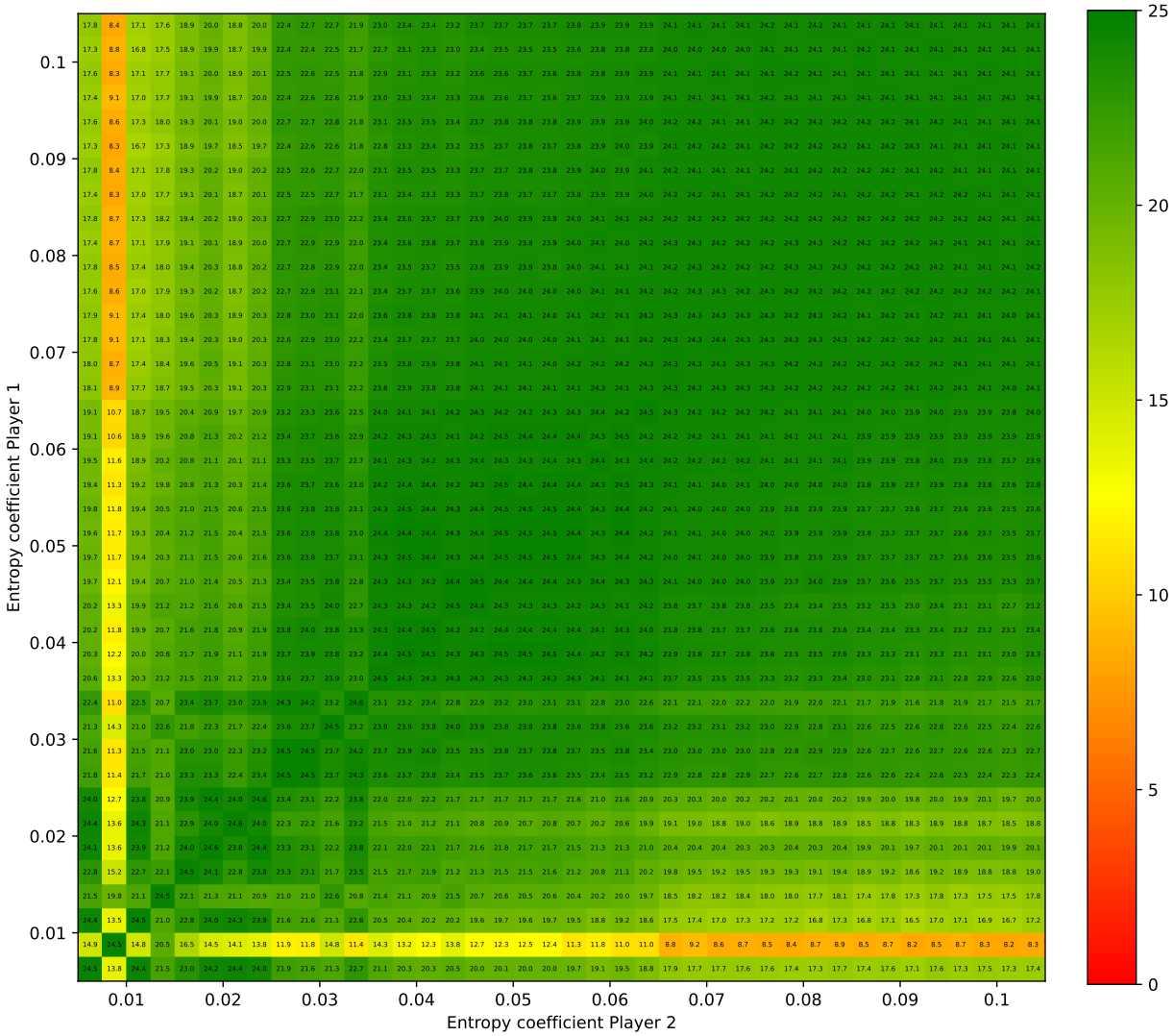

Figure 7. 2-Player Hanabi: XP matrix between public-private LSTM IPPO policies trained with different entropy coefficients. Four seeds per entropy coefficient $0.01, 0.02, ..., 0.10$.

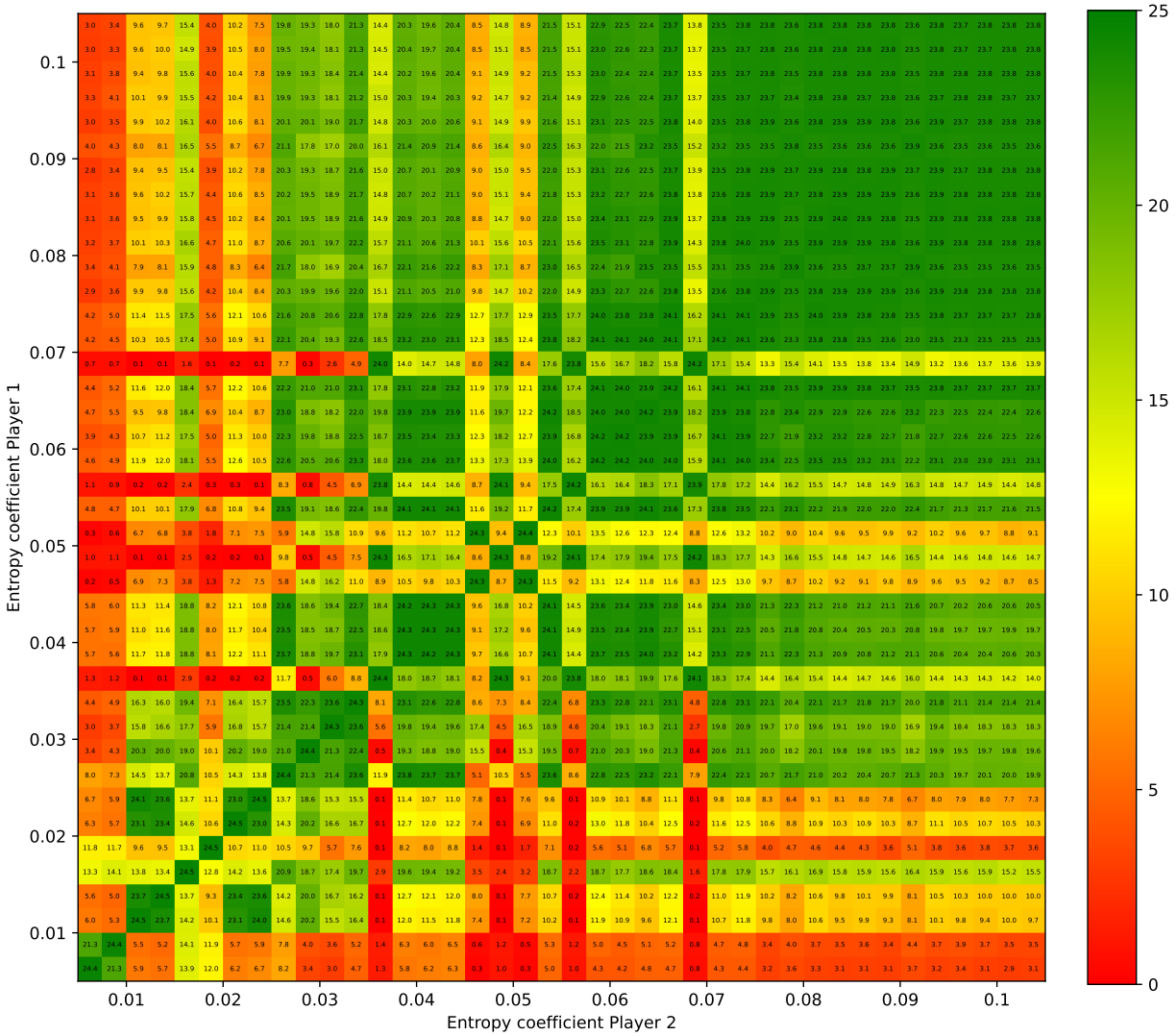

Figure 8. 2-Player Hanabi: XP matrix between feed-forward IPPO policies trained with different entropy coefficients. Four seeds per entropy coefficient $0.01, 0.02, ..., 0.10$.

D. Block XP Matrices in Overcooked

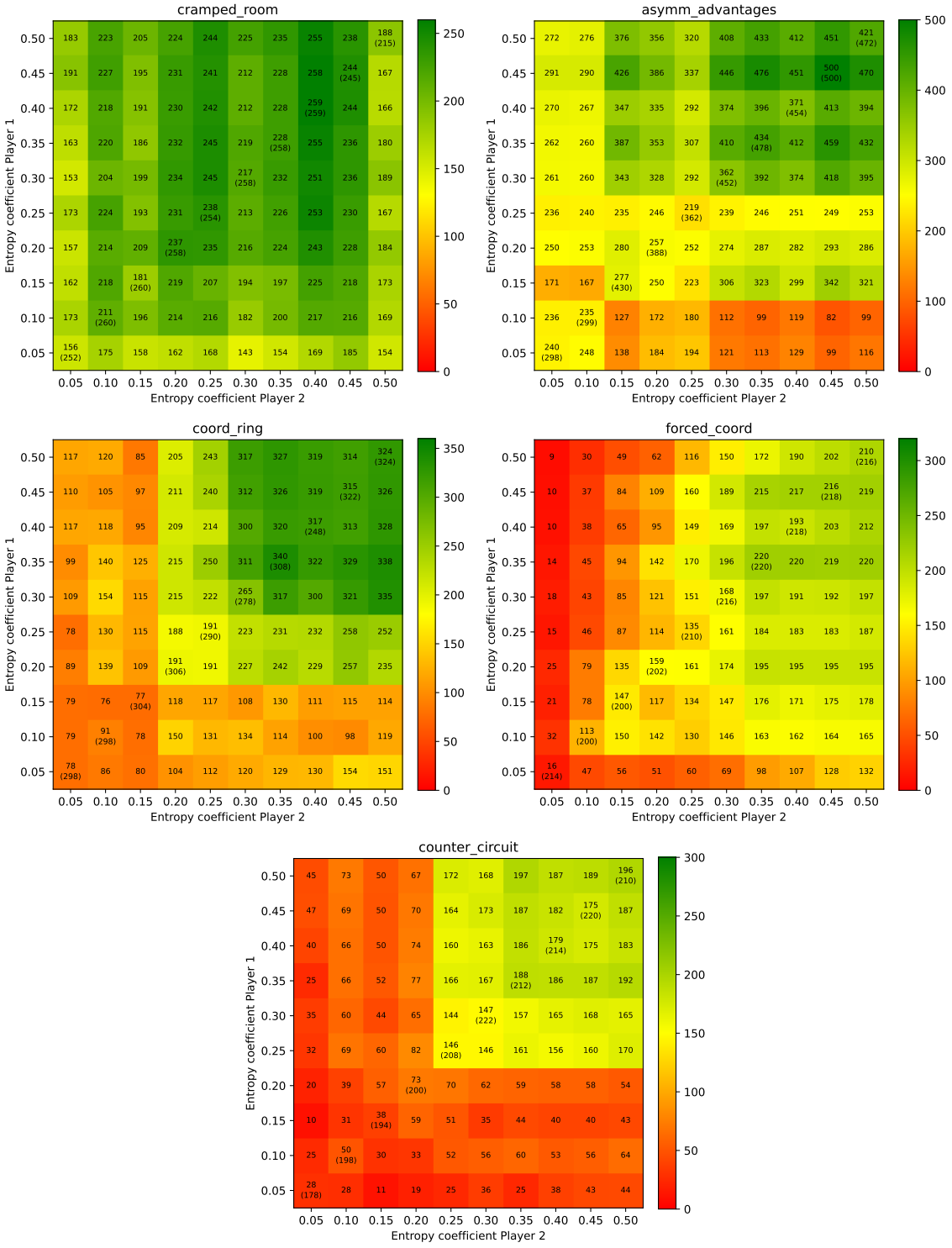

Figure 9. Overcooked: Block XP matrices for 100 greedified IPPO policies, for different entropy coefficients α, and $\lambda_{\text{GAE}} = 0.8$. Ten seeds per α. On the diagonal, the numbers are the average SP (in parentheses) and the average XP in the diagonal 10x10 blocks in which all the policies are trained with the same α. The off-diagonal numbers give the average XP in the off-diagonal 10x10 blocks, in which policies come from different α.